Measurement Analysis of Spatial and Temporal Correlation in Wideband Radio Channels with Adaptive Antenna Array

P. Karttunen[1], K. Kalliola[2], T. Laakso[1], and P. Vainikainen[2]

[1]Helsinki University of Technology
IRC/Laboratory of Telecommunications Technology
Otakaari 5A, FIN-02015 Espoo, Finland
E-mail: Petri.Karttunen@hut.fi,
Timo.Laakso@hut.fi

[2]Helsinki University of Technology
IRC/Radio Laboratory
Otakaari 5A, FIN-02015 Espoo, Finland
E-mail: kka@radio.hut.fi
pva@radio.hut.fi

ABSTRACT

This paper investigates the spatial and temporal correlation by measurements of an 8-element adaptive antenna array. The channel measurement data is gathered at a 2.154 GHz range outdoor radio channel. The measurement analysis is divided into three different categories: Investigation of spatial correlation between antenna elements at the base station (BS), spatial correlation of different mobile station (MS) locations and temporal correlation of the different multipath components. Also the differences in the correlation coefficient functions by using the complex-valued taps instead of the magnitude-valued taps are studied at the BS. The measurement analysis reveals that signals strongly correlate in the nearby BS antenna elements. However, at the different MS locations uncorrelated signals can be received when the physical separation is larger than half a wavelength. The multipath components in the impulse response profile become temporally uncorrelated after the excess delay values of 50 ns.

1. INTRODUCTION

One way to increase system capacity in future telecommunication systems is to employ adaptive antenna technologies. The adaptive antenna array processing techniques are sensitive to correlation properties of signals. Correlated signals exist especially in the uplink case (from MS to BS) where scattering near the MS is a common phenomenon. These signals have the tendency to impinge on the antenna within a small angular spread and therefore become correlated even for larger antenna separations [1]. When the correlation between elements is significant, the signals at different elements fade at the same time. Spatially strongly correlated signals make it difficult for the antenna processing methods to utilize the spatial structure of the channel. Thus, correlated fading reduces the performance of any diversity reception method.

In this paper, we examine the spatial and temporal correlation properties of a typical outdoor propagation radio channel based on the measurement data. The paper is organized as follows: Section 2 presents the mathematical model for the measured radio channel. In Section 3, the measurement system setup and the propagation environment are described. Section 4 analyzes the measurement results. Finally, in Section 5, the conclusions are drawn about the analysis results of the correlation properties of the channel.

2. CHANNEL MODEL

In this section the general multipath channel model and the correlation models are presented. The typical radio propagation environment is characterized by numerous propagation mechanisms like scattering from the nearby irregularly located buildings [2]. The radio channel model can be adequately described by the linear finite impulse response (FIR) filter model. The complex-valued impulse response of a time invariant wide-band channel can be expressed as

$$h(\tau) = \sum_{i=0}^{I-1} a_i e^{j\phi_i} \delta(\tau - \tau_i) \qquad (1)$$

where a_i is the path amplitude, ϕ_i is the path phase and τ_i is the path arrival delay with respect to the first arrived multipath component. The total number of resolved multipath components is denoted by I. Figure 1 illustrates the impulse response model. The multipath component is assumed to exist in the impulse response profile at the particular excess delay range $[\tau_i, \tau_{i+1}]$ if the total multipath power is greater than the detectable signal power of receiver. The different multipath components received during the bin duration cannot be resolved by the receiver and are merely either added or multiplied vectorially together [3][4].
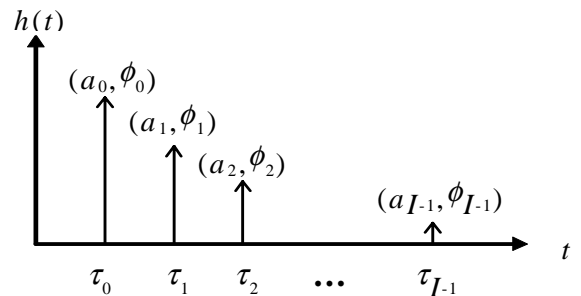

Figure 1 *Impulse response channel model*

The obtained channel tap values are defined for mathematical convenience as A_{pin} where p ($p=1, \ldots, P$) is the profile index, i ($i=1, \ldots, I$) is the excess delay in the given profile and n ($n=1, \ldots, N$) is the antenna element index. Figure 2 illustrates a possible variation of the tap values in the impulse responses at the measurement route. The small changes in the transmitter locations result only in small variations in the amplitude values of the individual multipath components. This small-scale signal fading governs the statistics of the amplitude variations of individual multipath components and is a prevailing phenomenon only in a small area ranging to distances of couple of wavelengths. A Rayleigh fading process has been typically used to model rapid small-scale amplitude fluctuations for non-line-of-sight (NLOS) environments or Rice distribution when specular or line-of-sight (LOS) component is present [4]. However, the empirical studies suggest that the behavior of the individual channel taps in the impulse response profiles can be still better explained by the log-normal statistics [4].
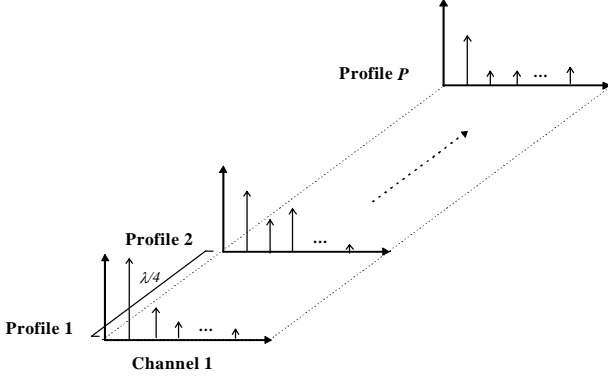
Figure 2 *Illustration of tap variations in the channel impulse responses along the measurement route*

Both the spatial and temporal correlation properties of multipath components have been explored by many authors, for example by Rappaport *et al.* in [5] and Dossi *et al.* in [6]. The correlation research work here has been refined by taking into account the complex valued taps and is especially extended to include the adaptive antenna arrays. Spatial correlation function measures the amplitude correlation between different antenna elements and is caused by the signal scattering around the transmitter as seen from the base station. The spatial correlation defines the level of correlation at two different antenna elements n and n' at the same excess delay index τ_i. The spatial correlation ρ_s between two linearly dependent random variables A_{pin} and $A_{pin'}$ which are either complex-valued or magnitude-valued can be computed from the formula of Pearson's correlation coefficient [7] as

$$\rho_s = \frac{\mathrm{E}\left[(A_{pin} - \overline{A}_{pin})(A_{pin'} - \overline{A}_{pin'})\right]}{\sqrt{\mathrm{E}\left[(A_{pin} - \overline{A}_{pin})^2\right]\mathrm{E}\left[(A_{pin'} - \overline{A}_{pin'})^2\right]}} \qquad (2)$$

Temporal correlation function measures the amplitude correlation between different excess delays τ_i and $\tau_{i'}$ in the same channel impulse response profile extracted from a particular antenna element. The temporal correlation is caused by propagation path differences of multipath components. The temporal correlation ρ_t between two linearly dependent random variables A_{pin} and $A_{pi'n}$ can be computed from a formula similar to Eq. (2) as

$$\rho_t = \frac{\mathrm{E}\left[(A_{pin} - \overline{A}_{pin})(A_{pi'n} - \overline{A}_{pi'n})\right]}{\sqrt{\mathrm{E}\left[(A_{pin} - \overline{A}_{pin})^2\right]\mathrm{E}\left[(A_{pi'n} - \overline{A}_{pi'n})^2\right]}} \qquad (3)$$

For the obtained correlation functions the exponentially decaying curves was fitted at the MS end

$$f(t) = Ae^{-Bt} - C \qquad (4)$$

where A, B and C are constants to be determined according to the minimum mean square error (MMSE) criterion [9]. The assumption of uniform scattering around the MS results in Bessel functions [2] which can be modeled by the exponential functions for small lag values. For generating exponentially correlated signals auto-regressive moving average (ARMA) models of different orders can be utilized.

3. MEASUREMENT SYSTEM

The used measurement system is based on a complex wideband radio channel sounder and a fast RF switch to record the channel impulse responses (IR) from multiple antenna elements [8]. The bandwidth of the receiver of the sounder is 100 MHz at carrier frequency of 2154 MHz. The chip frequency of the modulating pseudo noise (PN) code in the transmitter can be selected between 2.5 and 60 MHz. The received demodulated signal is divided into I and Q branches and sampled with two 120 Ms/s A/D - converters. The signal samples from every antenna element are then stored for off-line processing to obtain the complex IR of the channel. The length of a continuous measurement run is limited by the size of the memory buffer of the sampling card (currently 2×4 Mbytes for I and Q) and depends on the length of the used PN-code in the transmitter. The maximum number of recorded impulse responses is determined by the memory buffer of 8 Mbytes, which is used to store the signal samples before transferring to a hard disk.

BS antenna was connected to the receiver of the sounder through the element switching unit and located at a fixed position while the transmitter was positioned on a cart moving at a constant velocity. IRs were recorded from each element of the array while the cart was moving. The BS antenna array was a vertically polarized 8-element array of microstrip patch elements with $\lambda/2$ spacing. The beamwidth of the element limits the maximum viewable

sector of the array to approximately 120°. An omnidirectional discone antenna was used at the MS. The transmitter power level was 41.8 dBm. The measurement parameters are shown in Table 1.

Table 1 *Parameters of measurement system*

Parameter	Value
Carrier frequency	2154 MHz
Chip frequency of PN code	30 MHz
Sample rate	120 MHz
Code length	63
Delay resolution	33 ns
Delay window	2.1 μs
Element switching rate	238.1 kHz
Number of array elements	8
Samples / element / wavelength	4
Samples / element / m	28.7
MS speed	0.4 m/s
BS antenna height	11.5 m
MS antenna height	1.8 m
Number of measured array IRs	990
Length of MS Route	34.5 m

The measurements were carried out in the campus area of Helsinki university of technology (HUT) in Espoo, Finland. The BS antenna array was located on the roof of the 3-storey building of the Department of Electrical and Communications Engineering (see Figure 3). At the time of the measurement there were no moving objects in the environment other than the MS. The average distance from the transmitter to the receiver was 60 m.
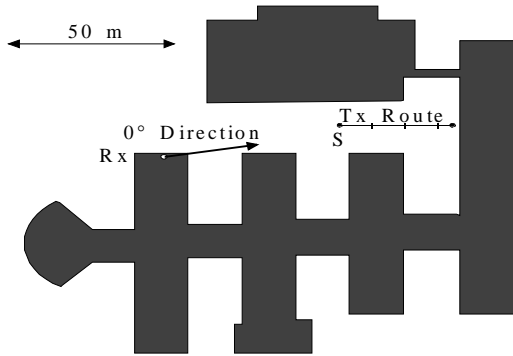

Figure 3 *Illustration of measurement site*

4. MEASUREMENT RESULTS

In this section both the spatial and temporal correlation properties are analyzed based on the measurement results. The measurement data is from the uniform linear array (ULA) antenna system where the first element has been used as the reference element. The threshold value of 25 dB from the maximum amplitude was set for each impulse response profile in order to remove correlated noise caused by the measurement system setup. The components left in the impulse response profile are the LOS component and the reflected components from the nearby wall. In the temporal correlation case the processing of the results has
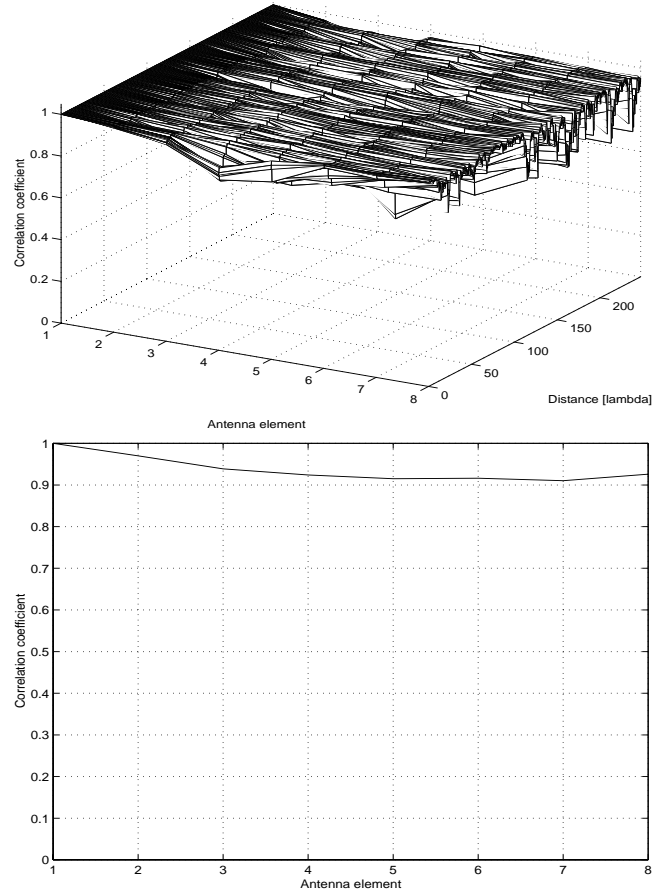

Figure 4 *Spatial correlation coefficient functions based on the magnitude values of the channel taps at the BS. a) Spatial correlation coefficient function as a function of antenna element index n and route distance b) Average spatial correlation coefficient function as a function of antenna element index n.*

been started from the first arrived multipath component, i.e., from the LOS component.

4.1 Spatial correlation at the BS end

Figure 4 shows the spatial correlation results between the antenna elements at the BS end. Eq. (2) was utilized for calculating the spatial correlation function. The absolute power value of each tap in the impulse responses was considered. The correlation is computed here by taking the impulse response values in each excess delay from the reference element and comparing them to the nearby elements in the array from each measurement point along the measurement route. Figure 4a) shows the spatial correlation function as a function of route distance and the physical antenna separation of $(n\text{-}1)\lambda/2$ wavelengths with respect to the reference element. The result plot shows that the correlation changes only very little as a function of the route distance. Figure 4b) shows the results when correlation coefficient functions have been averaged along the route. The resulting plots show that the spatial correlation function has strong correlation at short distances between antenna elements. High correlation is caused by the presence of LOS component in the impulse
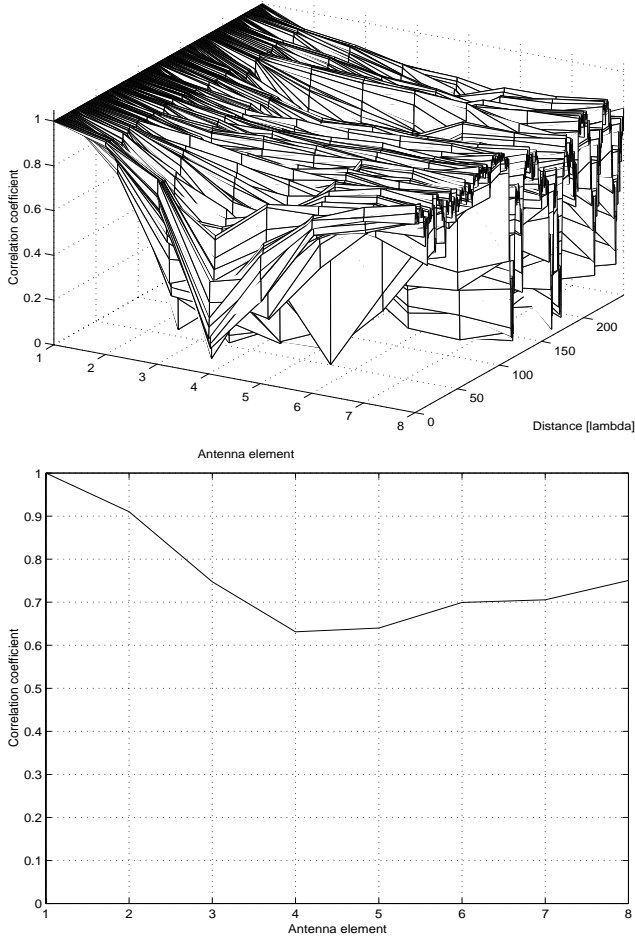
Figure 5 *Spatial correlation coefficient functions based on the complex channel taps at the BS. a) Spatial correlation coefficient function as a function of antenna element index n and route distance. b) Average spatial correlation coefficient function as a function of antenna element index n.*

Figure 6 *Spatial correlation coefficient functions based on the magnitude values of the channel taps at the MS end. A) Spatial correlation coefficient function as a function of distance and excess delay τ_i. b) Average spatial correlation coefficient function as a function of distance*

response profiles. The amplitude values of taps are more correlated than the complex-valued taps because the phase changes are more sensitive to the small changes in the transmitter locations. This effect is confirmed by the plots of Figure 5 where the same analysis was performed but with the complex-valued taps.

4.2 Spatial correlation at the MS end

Figure 6 shows the results for the spatial correlation at the MS end. The spatial correlation is calculated here as the correlation of magnitude-valued channel taps for profiles obtained at different locations with the same excess delays taken from the reference element. The obtained spatial correlation functions have been averaged along the measurement route. Figure 6a) shows the spatial correlation as a function of excess delay τ_i and the physical transmitter separation distance. The resulting plot show that the correlation values are naturally close to zero when there is no component in the particular excess delay. It can be also seen the existence of LOS and reflected components from the spatial correlation function as a higher correlation level. Figure 6b) shows the average
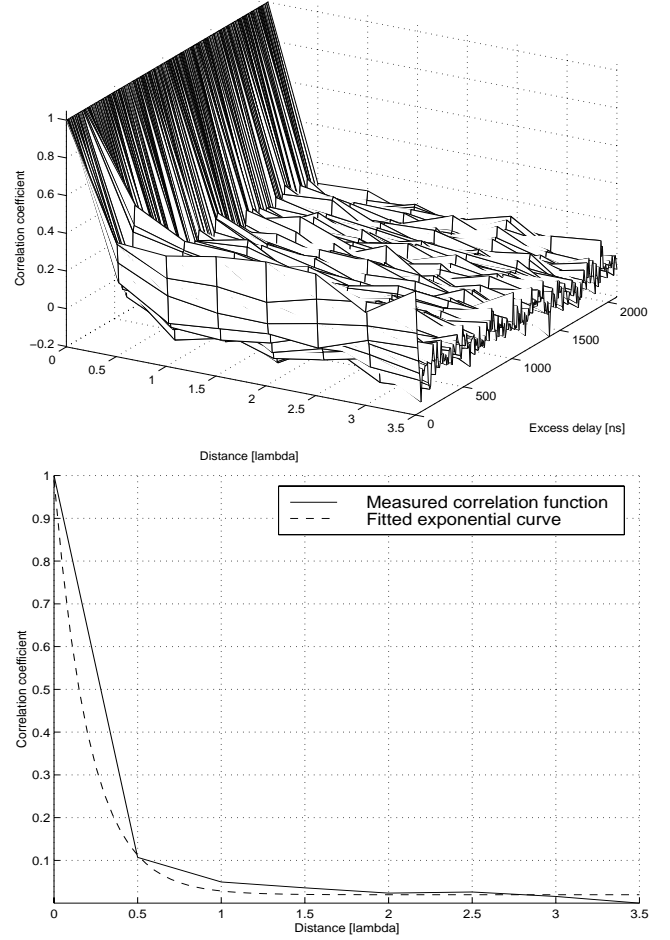
correlation function. The spatial correlation function has reduced to a very small correlation level after the physical distance of 0.5λ. The exponentially decaying correlation function has the parameters *A*=0.9706, *B*=2.3529 and *C*=-0.0196.

4.3 Temporal correlation

Figure 7 shows the results for the temporal correlation. The temporal correlation was computed from Eq. (3) where only the measurement data from the reference element was taken into account. The results for other antenna elements were similar and were not subsequently considered. The computation of the correlation function is accomplished by taking 7 measurement values encompassing one small-scale local area. The obtained correlation functions were averaged along each local area in the measurement route. Figure 7a) shows the temporal correlation function where the excess delay difference is defined as τ_i-$\tau_{i'}$, $i>i'$ and the excess delay as $\tau_{i'}$, $i'\geq0$. The excess delay τ_0 corresponds to first arrived multipath component. From the result plot it can be observed the presence of LOS and reflected components as higher

temporal correlation as a function of excess delay difference. The existence of the multipath components results in higher correlation values. Signal components in LOS case do not correlate after any excess delay values of 50 ns. Figure 7b) shows the temporal correlation function averaged along the excess delays τ_i. The X-axis grid spacing has been chosen to be the delay resolution of 33.3 ns. The reflected components do not have effect on the temporal correlation after the excess delay values of 25 ns. The exponentially fitted curve has the parameters A=0.9314, B=1.1765, C=-0.0588.

5. CONCLUSIONS

In this paper, the spatial and temporal correlation properties of the adaptive antenna array were studied. The results for the spatial correlation at the BS end confirm that strongly correlated signals exist in closely located antenna elements unless the antenna elements are widely separated. The correlation computation based on the magnitude-valued channel taps results in more correlated signals than the usage of the complex-valued channel taps. Spatial uncorrelateness at the MS end is already achieved after half a wavelength distance. Temporally uncorrelated signals are achieved after the excess delay values of 50 ns when the first LOS component has arrived at the excess delay value τ_0=0 ns. The signal components arriving after the LOS component become uncorrelated much faster, already after the excess delay values of 25 ns. These results for the spatial and the temporal correlation are in close agreement with those presented by Rappaport in [5].

ACKNOWLEDGEMENTS

REFERENCES

[1]   J. Salz and J. H. Winters, "Effect of fading correlation on adaptive arrays in digital mobile radio", *IEEE Trans. On Vehicular Technology*, Vol. 43, No. 4, Nov. 1994, pp. 1049-1057.

[2]   K. Pahlavan and A. H. Levesque, *Wireless Information Networks*, John Wiley & Sons, 1995, pp. 572.

[3]   H. Hashemi, "Simulation of the urban radio propagation channel", *IEEE Trans. on Vehicular Technology*, Vol. VT-28, No. 3, Aug, 1979, pp. 213-225.

[4]   H. Hashemi, "The Indoor radio propagation channel", *Proceedings of the IEEE*, Vol. 81, No. 7, July, 1993, pp. 943-968.

[5]   T. S. Rappaport, S. Y. Seidel and K. Takamizawa, "Statistical channel impulse response models for factory and open plan building radio communication system
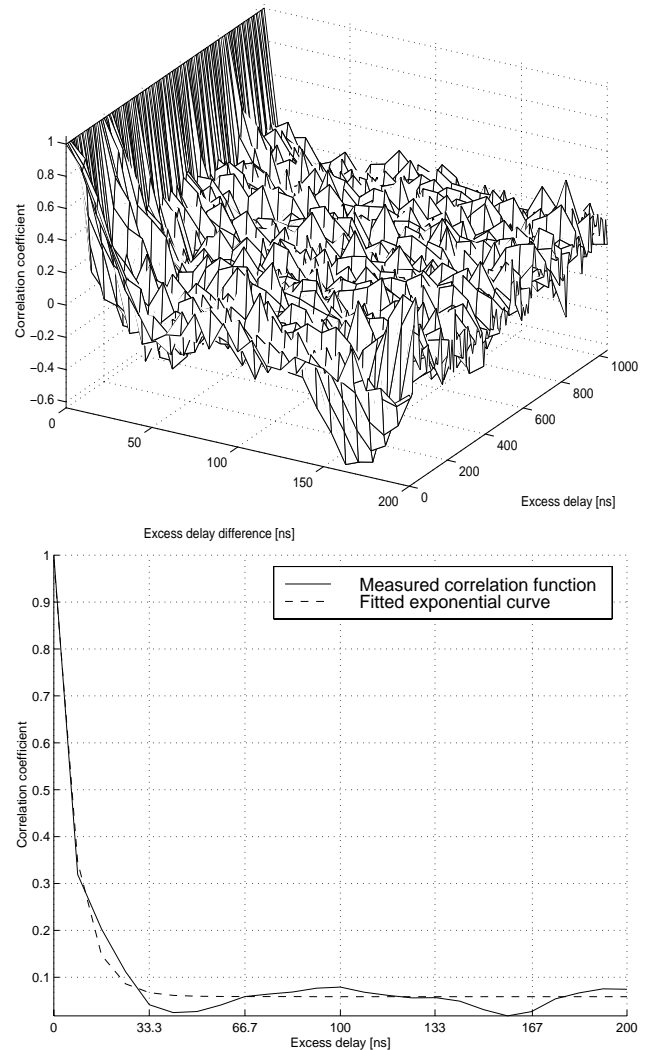
Figure 7 *Temporal correlation coefficient functions based on the magnitude values of the channel taps. a) Temporal correlation coefficient function as a function of excess delay difference and excess delay. b) Average temporal correlation coefficient function along the excess delays.*

Design", *IEEE Trans. On Communications*, Vol. 39, No. 5, May, 1991, pp. 794-806.

[6]   L. Dossi, G. Tartara and F. Tallone, "Statistical analysis of measured impulse response functions of 2.0 GHz indoor radio channels", *IEEE Journal on Selected Areas in Communications*, Vol. 14, No. 3, April, 1996, pp. 405-410.

[7]   J. S. Bendat and A. G. Piersol, *Random Data: Analysis and Measurement Procedures*, 2nd Edition, John Wiley & Sons, New York, 1986, pp. 566.

[8]   K. Kalliola and P. Vainikainen, "Characterization system for radio channel of adaptive array antennas", *Proceedings of 8th IEEE International Symposium on Personal, Indoor and Mobile Radio Communications*, Helsinki, Finland, September 1-4, 1997, pp. 95-99.

[9]   S. Haykin, *Adaptive Filter Theory*, 3rd edition, Prentice-Hall, 1996, pp. 989.